THE JOURNAL OF PHYSICAL CHEMISTRY Letters

pubs.acs.org/JPCL Letter

Understanding and Controlling the Performance-Limiting Steps of Catalyst-Modified Semiconductors

Nghi P. Nguyen, Brian L. Wadsworth, Daiki Nishiori, Edgar A. Reyes Cruz, and Gary F. Moore*

Cite This: J. Phys. Chem. Lett. 2021, 12, 199–203 Read Online

ACCESS | Metrics & More | Article Recommendations | Supporting Information

ABSTRACT: Understanding and controlling factors that restrict the rates of fuel-forming reactions are essential to designing effective catalyst-modified semiconductors for applications in solar-to-fuel technologies. Herein, we describe GaAs semiconductors featuring a polymeric coating that contains cobaloxime-type catalysts for photoelectrochemically powering hydrogen production. The activities of these electrodes (limiting current densities >20 mA cm^{-2} under 1-sun illumination) enable identification of fundamental performance-limiting bottlenecks encountered at relatively high rates of fuel formation. Experiments conducted under varying bias potential, pH, illumination intensity, and scan rate reveal two distinct mechanisms of photoelectrochemical hydrogen production. At relatively low polarization and pH, the limiting photoactivity is independent of illumination conditions and is attributed to a mechanism involving reduction of substrate protons. At relatively high polarization or pH, the limiting photoactivity shows a linear response to increasing photon flux and is attributed to a mechanism involving reduction of substrate water. This work illustrates the complex interplay between transport of photons, electrons, and chemical substrates in photoelectrosynthetic reactions and highlights diagnostic tools for better understanding these processes.

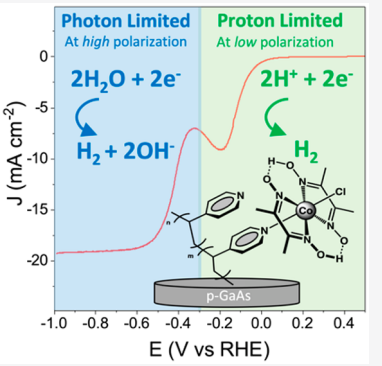

Advances in interfacial chemistry and rational synthetic design have accelerated development of catalyst-modified semiconductors that convert energy between photonic, electronic, and chemical forms.[1−10] These constructs hold promise for unleashing renewable-energy technologies that convert sunlight to fuels and other value-added chemical products. However, the ability to effectively interface the required light harvesting and catalytic components remains challenging as there is an incomplete understanding of how charges move through these materials and what the bottleneck rate-limiting steps are that restrict their performance.

In this report, we describe the synthesis, structural characterization, and photoelectrosynthetic properties of cobaloxime-polypyridyl-modified GaAs semiconductors (cobaloximePPyGaAs). The assemblies photoelectrochemically power hydrogen production at current densities that are among the highest reported for a molecular-catalyst-modified semiconductor,[11−16] achieving limiting current densities in excess of 20 mA cm^{-2} when under simulated 1-sun illumination, and related rates of fuel production greater than 100 nmol H_2 cm^{-2} s^{-1}. These activities enable experiments that provide physical insights regarding reaction mechanisms and fundamental performance-limiting factors encountered at accelerated fuel-formation rates. Although these studies make specific use of GaAs semiconductors interfaced with cobaloxime-type catalysts, the key findings and discussions are likely relevant to other materials and chemical transformations involving proton-transfer reactions. Thus, the photoelectrochemical techniques highlighted in this report (including applications of varying electrochemical polarization, pH, illumination intensity, and scan rate) provide a general yet useful strategy for better understanding, and ultimately controlling, the performance of catalyst-modified semiconductors.

Our use of GaAs semiconductors in this current work was prompted by studies of related molecular-catalyst-modified GaP electrodes.[17−23] When these GaP-based constructs were illuminated at 1-sun intensity, the hydrogen evolution reaction (HER) activities were not limited by a chemical step (i.e., chemical catalysis/energy storage) but instead were limited by the incident photon flux and kinetics associated with charge transport (i.e., light capture and conversion steps).[18] These findings indicate that increasing the illumination intensity, or utilizing a semiconductor component that can harvest a larger portion of the solar spectrum, could enhance fuel-forming reaction rates. Based on their respective band gaps, GaAs can harvest photons with wavelengths up to 870 nm, while GaP can only absorb photons with wavelengths up to 549 nm (Figure 1a). Thus, if the overall incident photon-to-current efficiencies are similar, we hypothesize that GaAs-based

Received: August 5, 2020
Accepted: October 27, 2020

https://dx.doi.org/10.1021/acs.jpclett.0c02386
J. Phys. Chem. Lett. 2021, 12, 199−203

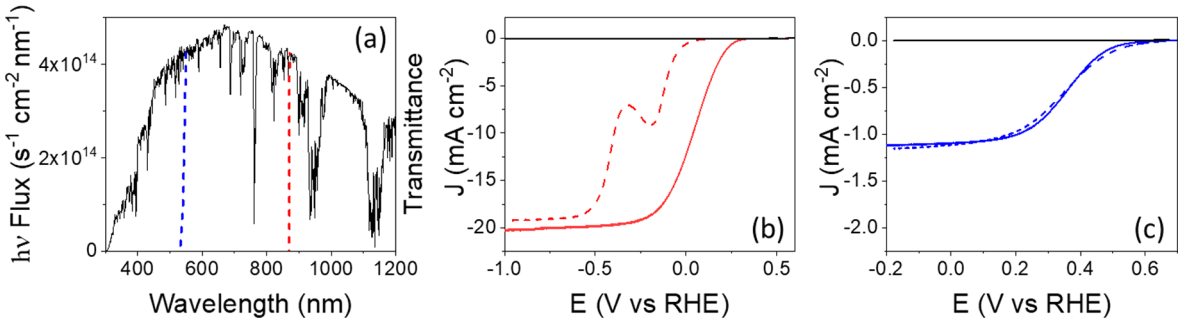

Figure 1. (a) The air mass 1.5 global tilt solar flux spectrum (black solid) as well as transmission spectra of the GaP (bandgap = 2.26 eV) (blue dash) and GaAs (bandgap = 1.43 eV) (red dash) semiconductors used in this work. (b) Linear sweep voltammograms recorded at a scan rate of 100 mV s^{-1} using cobaloxime-polypyridyl-modified GaAs (cobaloximeIPPyIGaAs) electrodes in pH 7 (dash traces) or pH 13 (solid traces) solutions under simulated 1-sun illumination (red traces) or in the dark (black traces). (c) Linear sweep voltammograms recorded at a scan rate of 100 mV s^{-1} using cobaloxime-polypyridyl-modified GaP (cobaloximeIPPyIGaP) electrodes in pH 7 (dash traces) or pH 13 (solid traces) solutions under simulated 1-sun illumination (blue traces) or in the dark (black traces).

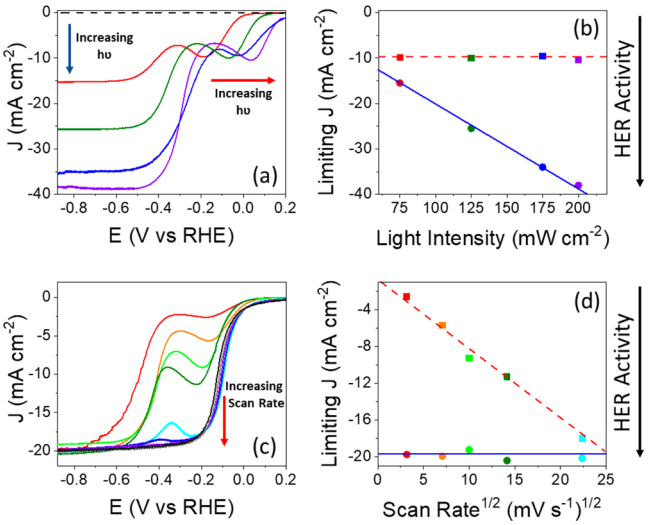

Figure 2. (a) Linear sweep voltammograms recorded at 100 mV s^{-1} using cobaloximeIPPyIGaAs electrodes in 0.1 M phosphate buffer (pH 7) and the following illumination intensities: 0 (black dash), 75 (red), 125 (olive), 175 (blue), and 200 (violet) mW cm^{-2}. (b) Plots of the limiting current densities recorded in the low polarization region (squares) and high polarization region (circles) versus the illumination intensity. (c) Linear sweep voltammograms recorded under 100 mW cm^{-2} illumination using cobaloximeIPPyIGaAs electrodes in 0.1 M phosphate buffer (pH 7) and the following scan rates: 10 (red), 50 (orange), 100 (green), 200 (olive), 500 (cyan), 700 (blue), 1000 (violet), 1200 (gray), and 1500 (black) mV s^{-1}. (d) Plots of the limiting current densities recorded in the low polarization region (squares) and high polarization region (circles) versus the scan rate.

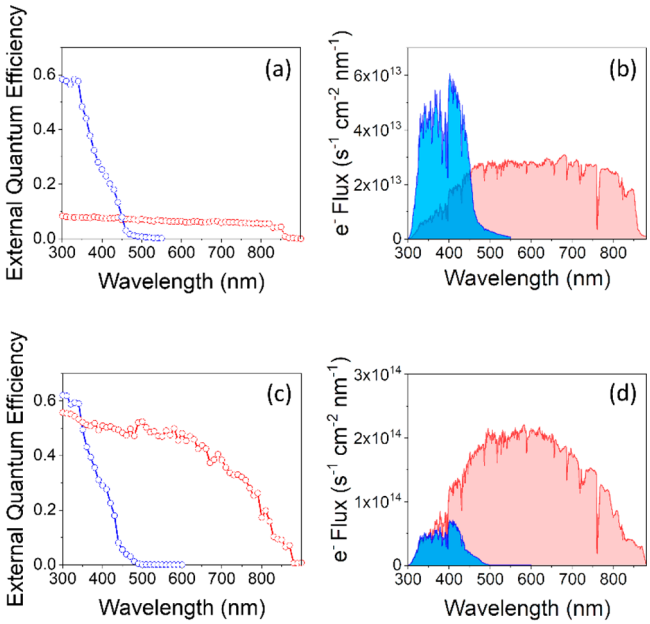

Figure 3. (a) EQE action spectra recorded at pH 7 using either cobaloximeIPPyIGaAs (red) or cobaloximeIPPyIGaP (blue) working electrodes polarized at 0 V vs RHE. (b) Electron flux spectra for cobaloximeIPPyIGaAs (red) and cobaloximeIPPyIGaP (blue) calculated using the EQE action spectra shown in Figure 3a and the solar flux spectrum shown in Figure 1a. (c) EQE action spectra recorded at pH 13 using either cobaloximeIPPyIGaAs (red) or cobaloximeIPPyIGaP (blue) working electrodes polarized at 0 V vs RHE. (d) Electron flux spectra for cobaloximeIPPyIGaAs (red) and cobaloximeIPPyIGaP (blue) calculated using the EQE action spectra shown in Figure 3c and the solar flux spectrum shown in Figure 1a.

constructs should achieve higher current densities and deliver charge carriers required for activating surface-immobilized catalysts at faster rates.

Synthesis of cobaloximeIPPyIGaAs assemblies was achieved via modification of a method previously developed for functionalizing GaP,[17,20,21] and structural characterization (including contact angle measurements, ellipsometry, inductively coupled plasma mass spectrometry, X-ray photoelectron spectroscopy, and grazing angle attenuated total reflectance Fourier transform infrared spectroscopy) provides converging lines of evidence for successful functionalization of the GaAs substrates (see Supporting Information). Voltammograms recorded using cobaloximeIPPyIGaAs, polypyridyl-modified GaAs (PPyIGaAs), and GaAs working electrodes immersed in 0.1 M phosphate buffered aqueous solutions (pH 7) are shown in Figures 1b and S22. Under simulated 1-sun illumination (100 mW cm^{-2}), the cobaloximeIPPyIGaAs electrodes produce a current density of 1.0 ± 0.4 mA cm^{-2} when polarized at the H^+/H_2 equilibrium potential, and achieve a limiting current density of ~20 mA cm^{-2} when polarized at more negative potentials. For comparison, when studied under otherwise identical experimental conditions, the analogous GaP-based constructs (cobaloximeIPPyIGaP) achieve a current density of 1.08 ± 0.03 mA cm^{-2} when polarized at the H^+/H_2 equilibrium potential, and approach a

https://dx.doi.org/10.1021/acs.jpclett.0c02386
J. Phys. Chem. Lett. 2021, 12, 199−203

limiting current density that remains at ∼1 mA cm^{-2} when polarizing to more negative potentials (Figure 1c).

Unlike the voltammograms recorded using cobaloxime|PPy|GaP electrodes, which display single S-shaped waveforms, the voltammograms recorded using cobaloxime|PPy|GaAs electrodes in pH neutral aqueous solutions display two distinct regions of photoelectrosynthetic performance (i.e., dual-waveform voltammograms featuring two limiting current features). We term the region of photoelectrosynthetic performance at less negative bias potentials the *low polarization region,* and the region of photoelectrosynthetic performance at more negative bias potentials the *high polarization region*. The low polarization region spans from approximately −0.3 V vs RHE to more positive potentials and includes a limiting current peak feature centered at −0.2 V vs RHE, with an intensity of ∼10 mA cm^{-2}, in voltammograms recorded at pH 7 under 100 mW cm^{-2} illumination. Sweeping the polarization to potentials negative of this peak feature results in decreasing currents (i.e., rates of charge transfer) despite the increasing applied bias potential. This result indicates that transport, and thus local concentration, of substrates other than electrons begins to limit the HER activity.[24] Conversely, in the high polarization region, which spans from approximately −0.3 V vs RHE to more negative potentials, the current response switches back to increasing with further negative polarization until reaching a limiting value that approaches ∼20 mA cm^{-2}.

To further explore the dual-waveform nature associated with the GaAs-based assemblies, photoelectrochemical experiments were also performed at elevated pH. Voltammograms recorded using cobaloxime|PPy|GaAs electrodes immersed in 0.1 M NaOH aqueous solutions (pH 13) are shown in Figures 1b and S22. Under these conditions, the cobaloxime|PPy|GaAs electrodes produce a current density of 10 ± 1 mA cm^{-2} when polarized at the H^+/H_2 equilibrium potential, and the current density steadily increases upon polarizing to more negative potentials until reaching a limiting value that again approaches ∼20 mA cm^{-2}. In addition, the voltammograms recorded under basic conditions display a single S-shaped waveform (Figures 1b, S22b, and S25) and not the dual waveform observed in experiments performed at pH 7 (Figures 2 and S26). For comparison, at pH 13 and otherwise identical experimental conditions, the analogous cobaloxime|PPy|GaP assemblies achieve a current density of only 1.08 ± 0.03 mA cm^{-2} when polarized at the H^+/H_2 equilibrium potential, and display a limiting current density that remains at ∼1 mA cm^{-2} when polarizing to more negative potentials (Figure 1c). Thus, unlike cobaloxime|PPy|GaAs, the current response versus the RHE potential (which adjusts for the nernstian pH response of the HER) shows relatively little to no difference in experiments performed at pH 7 versus 13 when using cobaloxime|PPy|GaP working electrodes.[21,25,26]

The observation of dual-waveform voltammograms and changes in waveforms as a function of pH have been reported by Gerischer et al. in experiments involving unmodified-GaAs electrodes interfaced with a liquid electrolyte.[27] The authors proposed that currents at lower bias potentials are restricted by diffusion of solvated protons to the electrode surface, and at higher bias potentials the reduction of water becomes limited by the number of electron−hole pairs generated via illumination of the semiconductor.[27] To investigate if similar mechanisms are at play when using cobaloxime|PPy|GaAs, we analyzed their photoelectrosynthetic performance under varying illumination intensity and scan rate.

At pH 7, the limiting current at lower polarization is independent of illumination conditions when modifying them from 75 up to 200 mW cm^{-2} (Figures 2a and b). However, the position of the peak feature shifts toward more positive potentials when increasing the light intensity. Juxtaposed to this invariance of the limiting current intensity in the low polarization region when modifying the illumination conditions, its value does increase when modifying the scan rate from 10 up to 500 mV s^{-1} (Figure 2c and d), whereupon the limiting current becomes scan rate independent and saturates at a current density similar to that recorded at higher polarization (∼20 mA cm^{-2}) (Figure S23). These results are consistent with limitations of the HER activity in the low polarization region due to diffusion of substrate protons (the second step in eq 1). The apparent shift of the current limiting peak feature to more positive potentials when increasing the illumination intensity is attributed to a more rapid consumption of substrate protons at higher light fluxes. In other words, the catalytic turnover frequency increases at higher illumination intensities and the concentration of protons at the electrode surface becomes depleted earlier in the voltammogram scan, causing the peak feature to appear at more positive potentials. Conversely, the relative thickness of the diffusion layer, which is the region in the vicinity of an electrode where concentrations of chemical substrates are different from their values in the bulk solution,[28] depends on the time scale of the voltammogram scan. At faster scan rates, the thickness of the diffusion layer is narrower, enabling higher fluxes of chemical substrate to the electrode surface and hence higher currents.[29,30]

In the high polarization region, the response of the limiting current to increasing light intensity and scan rate is counter to that observed in the low polarization region (Figure 2b and d), and the limiting current is instead proportional to the illumination intensity yet invariant to increasing scan rate. These results are consistent with limitations of the HER activity related to the availability of photons at the electrode surface (the first step in eq 2). Under simulated 1-sun illumination, increasing the scan rate to improve mass transport, and thereby increase the availability of protons at the electrode surface, does not increase the limiting current and HER activity at high polarization because the electrode is photon starved. Further, at relatively high polarization, or high pH (Figures S24 and S25), the concentration of protons at the electrode surface is relatively low and water serves as a weak acid and reactant (the second step in eq 2).

Reduction of protons at relatively low polarization and low pH:

$$\text{Step 1: } h\nu + \text{semiconductor} \rightarrow e^- + h^+$$

$$\text{Step 2: } 2H^+ + 2e^- \rightarrow H_2 \quad (1)$$

Reduction of water at relatively high polarization or high pH:

$$\text{Step 1: } h\nu + \text{semiconductor} \rightarrow e^- + h^+$$

$$\text{Step 2: } 2H_2O + 2e^- \rightarrow H_2 + 2OH^- \quad (2)$$

External quantum efficiency (EQE) action spectra provide information on the number of charge carriers collected as current versus the number of photons incident on the working electrode surfaces. Analyses of the EQE action spectra recorded using cobaloxime|PPy|GaAs electrodes polarized at

https://dx.doi.org/10.1021/acs.jpclett.0c02386
J. Phys. Chem. Lett. 2021, 12, 199−203

0 V vs RHE (Figures 3a–d and S22) confirm these constructs are photoactive over wavelengths ranging from 300 to 870 nm. Conversely, cobaloxime|PPy|GaP electrodes are only photoactive over wavelengths ranging from 300 to 549 nm (Figure 3a–d). In addition, gas chromatography analyses of headspace gas samples taken from photoelectrochemical cells equipped with cobaloxime|PPy|GaAs working electrodes polarized for 20 min at potentials in the high polarization region or low polarization region, and at pH 7 or 13, all confirm the production of hydrogen gas with near unity faradaic efficiency (Figure S29). These results corroborate our hypothesis that in comparison with the analogous GaP-based constructs, the GaAs-based constructs should be capable of delivering charge carriers required for activating surface-immobilized catalysts at significantly faster rates and thereby facilitate mechanistic studies at relatively high rates of fuel formation.

In conclusion, the higher activities achieved using the GaAs-based assemblies enable identification of the performance-limiting factors encountered at accelerated fuel-formation rates and reveal a hitherto unexplored switching of the rate-limiting steps and reagents required for driving photoelectrosynthetic reactions. In a longer-term view, a viable photoelectrosynthetic device must be efficient, durable, and ultimately cost-effective. To date, no assembly effectively achieves this. Thus, there is a need for ongoing research addressing all of these aspects. The results described in this Letter highlight the modularity of a polymeric-attachment strategy and provide insights for better understanding and controlling the rate-limiting steps of fuel-forming reactions at catalyst-modified semiconductors where photons, electrons, and protons are all required reagents.

■ ASSOCIATED CONTENT

Supporting Information

The Supporting Information is available free of charge at https://pubs.acs.org/doi/10.1021/acs.jpclett.0c02386.

Experimental methods and additional results and data (PDF)

■ AUTHOR INFORMATION

Corresponding Author

Gary F. Moore − *School of Molecular Sciences and the Biodesign Institute Center for Applied Structural Discovery (CASD), Arizona State University, Tempe, Arizona 85287-1604, United States;* orcid.org/0000-0003-3369-9308; Email: gfmoore@asu.edu

Authors

Nghi P. Nguyen − *School of Molecular Sciences and the Biodesign Institute Center for Applied Structural Discovery (CASD), Arizona State University, Tempe, Arizona 85287-1604, United States*

Brian L. Wadsworth − *School of Molecular Sciences and the Biodesign Institute Center for Applied Structural Discovery (CASD), Arizona State University, Tempe, Arizona 85287-1604, United States;* orcid.org/0000-0002-0274-9993

Daiki Nishiori − *School of Molecular Sciences and the Biodesign Institute Center for Applied Structural Discovery (CASD), Arizona State University, Tempe, Arizona 85287-1604, United States*

Edgar A. Reyes Cruz − *School of Molecular Sciences and the Biodesign Institute Center for Applied Structural Discovery (CASD), Arizona State University, Tempe, Arizona 85287-1604, United States*

Complete contact information is available at: https://pubs.acs.org/10.1021/acs.jpclett.0c02386

Notes

The authors declare no competing financial interest.

■ ACKNOWLEDGMENTS

This work was supported by the National Science Foundation under Early Career Award 1653982 (polymeric surface chemistry) and by the U.S. Department of Energy, Office of Science, Office of Basic Energy Sciences, under Early Career Award DE-SC0021186 (light intensity experiments). G.F.M. acknowledges support from the Camille Dreyfus Teacher-Scholar Awards Program. B.L.W. was supported by an IGERT-SUN fellowship funded by the National Science Foundation (1144616) and the Phoenix Chapter of the ARCS Foundation. The authors gratefully acknowledge Diana Convey in the Goldwater Materials Science Facility at Arizona State University for assistance with ellipsometry measurements, Gwyneth Gordon in the Metals, Environmental and Terrestrial Analytical Laboratory at Arizona State University for assistance with ICP-MS measurements, Timothy Karcher in the Eyring Materials Center at Arizona State University for assistance with XPS data collection, and Michael Dodson in the Biodesign Institute at Arizona State University for assistance with contact angle measurements.

■ REFERENCES

(1) Ardo, S.; Fernandez Rivas, D. F.; Modestino, M. A.; Schulze Greiving, V. S.; Abdi, F. F.; Alarcon Llado, E. A.; Artero, V.; Ayers, K.; Battaglia, C.; Becker, J.-P.; et al. Pathways to Electrochemical Solar-Hydrogen Technologies. *Energy Environ. Sci.* **2018**, *11*, 2768–2783.

(2) Faunce, T. A.; Lubitz, W.; Rutherford, A. W.; MacFarlane, D.; Moore, G. F.; Yang, P.; Nocera, D. G.; Moore, T. A.; Gregory, D. H.; Fukuzumi, S.; et al. Energy and Environment Policy Case for a Global Project on Artificial Photosynthesis. *Energy Environ. Sci.* **2013**, *6*, 695–698.

(3) Blankenship, R. E.; Tiede, D. M.; Barber, J.; Brudvig, G. W.; Fleming, G.; Ghirardi, M.; Gunner, M. R.; Junge, W.; Kramer, D. M.; Melis, A.; et al. Comparing Photosynthetic and Photovoltaic Efficiencies and Recognizing the Potential for Improvement. *Science* **2011**, *332*, 805–809.

(4) Walter, M. G.; Warren, E. L.; McKone, J. R.; Boettcher, S. W.; Mi, Q.; Santori, E. A.; Lewis, N. S. Solar Water Splitting Cells. *Chem. Rev.* **2010**, *110*, 6446–6473.

(5) Gray, H. B. Powering the Planet with Solar Fuel. *Nat. Chem.* **2009**, *1*, 7.

(6) Khan, M. A.; Varadhan, P.; Ramalingam, V.; Fu, H.; Idriss, H.; He, J. Importance of Oxygen Measurements during Photoelectrochemical Water-Splitting Reactions. *ACS Energy Lett.* **2019**, *4*, 2712–2718.

(7) Holm, J. V.; Jørgensen, H.; Krogstrup, P.; Nygard, J.; Liu, H.; Aagesen, M. Surface-passivated GaAsP single-nanowire solar cells exceeding 10% efficiency grown on silicon. *Nat. Commun.* **2013**, *4*, 1–5.

(8) Lewis, N. S.; Nocera, D. G. Powering the Planet: Chemical Challenges in Solar Energy Utilization. *Proc. Natl. Acad. Sci. U. S. A.* **2006**, *103*, 15729–15735.

(9) Wang, Y.; Wei, H.; Lv, H.; Chen, Z.; Zhang, J.; Yan, X.; Lee, L.; Wang, Z. M.; Chueh, Y. Highly Stable Three-Dimensional Nickel-Cobalt Hydroxide Hierarchical Heterostructures Hybridized with Carbon Nanotubes for High-Performance Energy Storage Devices. *ACS Nano* **2019**, *13*, 11235–11248.

(10) Manikandan, A.; Lee, L.; Wang, Y.; Chen, C.; Chen, Y.; Medina, H.; Tseng, J.; Wang, Z. M.; Chueh, Y. Graphene-coated copper nanowire networks as a highly stable transparent electrode in harsh environments toward efficient electrocatalytic hydrogen evolution reactions. *J. Mater. Chem. A* **2017**, *5*, 13320−13328.
(11) Gu, J.; Yan, Y.; Young, J. L.; Steirer, K. X.; Neale, N. R.; Turner, J. A. Water Reduction by a p-$GaInP_2$ Photoelectrode Stabilized by an Amorphous TiO_2 Coating and a Molecular Cobalt Catalyst. *Nat. Mater.* **2016**, *15*, 456−460.
(12) Zhao, Y.; Anderson, N. C.; Ratzloff, M. W.; Mulder, D. W.; Zhu, K.; Turner, J. A.; Neale, N. R.; King, P. W.; Branz, H. M. Proton Reduction Using a Hydrogenase-Modified Nanoporous Black Silicon Photoelectrode. *ACS Appl. Mater. Interfaces* **2016**, *8*, 14481−14487.
(13) Hou, Y.; Abrams, B. L.; Vesborg, P. C.; Björketun, M. E.; Herbst, K.; Bech, L.; Setti, A. M.; Damsgaard, C. D.; Pedersen, T.; Hansen, O.; et al. Bioinspired Molecular Co-Catalysts Bonded to a Silicon Photocathode for Solar Hydrogen Evolution. *Nat. Mater.* **2011**, *10*, 434−438.
(14) Zhang, B.; Sun, L. Artificial Photosynthesis: Opportunities and Challenges of Molecular Catalysts. *Chem. Soc. Rev.* **2019**, *48*, 2216−2264.
(15) Dalle, K. E.; Warnan, J.; Leung, J. J.; Reuillard, B.; Karmel, I. S.; Reisner, E. Electro- and Solar-Driven Fuel Synthesis with First Row Transition Metal Complexes. *Chem. Rev.* **2019**, *119*, 2752−2875.
(16) Queyriaux, N.; Kaeffer, N.; Morozan, A.; Chavarot-Kerlidou, M.; Artero, V. Molecular Cathode and Photocathode Materials for Hydrogen Evolution in Photoelectrochemical Devices. *J. Photochem. Photobiol., C* **2015**, *25*, 90−105.
(17) Krawicz, A.; Yang, J.; Anzenberg, E.; Yano, J.; Sharp, I. D.; Moore, G. F. Photofunctional Construct that Interfaces Molecular Cobalt-Based Catalysts for H_2 Production to a Visible-Light-Absorbing Semiconductor. *J. Am. Chem. Soc.* **2013**, *135*, 11861−11868.
(18) Wadsworth, B. L.; Beiler, A. M.; Khusnutdinova, D.; Reyes Cruz, E. A.; Moore, G. F. Interplay between Light Flux, Quantum Efficiency, and Turnover Frequency in Molecular-Modified Photoelectrosynthetic Assemblies. *J. Am. Chem. Soc.* **2019**, *141*, 15932−15941.
(19) Moore, G. F.; Sharp, I. D. A Noble-Metal-Free Hydrogen Evolution Catalyst Grafted to Visible Light-Absorbing Semiconductors. *J. Phys. Chem. Lett.* **2013**, *4*, 568−572.
(20) Beiler, A. M.; Khusnutdinova, D.; Wadsworth, B. L.; Moore, G. F. Cobalt Porphyrin−Polypyridyl Surface Coatings for Photoelectrosynthetic Hydrogen Production. *Inorg. Chem.* **2017**, *56*, 12178−12185.
(21) Cedeno, D.; Krawicz, A.; Doak, P.; Yu, M.; Neaton, J. B.; Moore, G. F. Using Molecular Design to Control the Performance of Hydrogen-Producing Polymer-Brush-Modified Photocathodes. *J. Phys. Chem. Lett.* **2014**, *5*, 3222−3226.
(22) Beiler, A. M.; Khusnutdinova, D.; Jacob, S. I.; Moore, G. F. Solar Hydrogen Production Using Molecular Catalysts Immobilized on Gallium Phosphide (111)A and (111)B Polymer-Modified Photocathodes. *ACS Appl. Mater. Interfaces* **2016**, *8*, 10038−10047.
(23) Beiler, A. M.; Khusnutdinova, D.; Jacob, S. I.; Moore, G. F. Chemistry at the Interface: Polymer-Functionalized GaP Semiconductor for Solar Hydrogen Production. *Ind. Eng. Chem. Res.* **2016**, *55*, 5306−5314.
(24) Santangelo, P. G.; Miskelly, G. M.; Lewis, N. S. Voltammetry of Semiconductor Electrodes. 2. Cyclic Voltammetry of Freely Diffusing Redox Species and Rotating Semiconductor Disk Voltammetry. *J. Phys. Chem.* **1989**, *93*, 6128−6136.
(25) Electrochemical studies under acidic conditions were not performed due to the instability of cobaloximes at low pH.
(26) Artero, V.; Fontecave, M. Some general principles of designing electrocatalysts with hydrogenase activity. *Coord. Chem. Rev.* **2005**, *249*, 1518−1535.
(27) Gerischer, H.; Muller, N.; Haas, O. On the Mechanism of Hydrogen Evolution at GaAs Electrodes. *J. Electroanal. Chem. Interfacial Electrochem.* **1981**, *119*, 41−48.
(28) IUPAC. *Compendium of Chemical Terminology*, 2nd ed. (the "Gold Book"); McNaught, A. D., Wilkinson, A.; Blackwell Scientific Publications: Oxford, 1997. Online version (2019) created by S. J. Chalk.
(29) Bard, A. J.; Faulkner, L. R. Chapter 6: Potential Sweep Methods. In *Electrochemical Methods: Fundamentals and Applications*, 2nd ed.; John Wiley & Sons: New York, 2001.
(30) Costentin, C.; Saveant, J.-M. Multielectron, Multistep Molecular Catalysis of Electrochemical Reactions: Benchmarking of Homogeneous Catalysts. *ChemElectroChem* **2014**, *7*, 1226−1236.

https://dx.doi.org/10.1021/acs.jpclett.0c02386
J. Phys. Chem. Lett. 2021, 12, 199−203